APPLIED GEOPHYSICS, Vol.11, No.4 (December 2014), P. 429-436, 10 Figures.
DOI: 10.1007/s11770-014-0450-4

Discriminating between explosions and earthquakes

Cho, Kwang-Hyun[1]

Abstract: Earthquake, explosion, and a nuclear test data are compared with forward modeling and band-pass filtered surface wave amplitude data for exploring methodologies to improve earthquake–explosion discrimination. The proposed discrimination method is based on the solutions of a double integral transformation in the wavenumber and frequency domains. Recorded explosion data on June 26, 2001 (39.212°N, 125.383°E) and October 30, 2001 (38.748°N, 125.267°E), a nuclear test on October 9, 2006 (41.275°N, 129.095°E), and two earthquakes on April 14, 2002 (39.207°N, 125.686°E) and June 7, 2002 (38.703°N, 125.638°E), all in North Korea, are used to discriminate between explosions and earthquakes by seismic wave analysis and numerical modeling. The explosion signal is characterized by first P waves with higher energy than that of S waves. Rg waves are clearly dominant at 0.05 –0.5 Hz in the explosion data but not in the earthquake data. This feature is attributed to the dominant P waves in the explosion and their coupling with the SH components.
Keywords: explosion, earthquake, nuclear test, P wave, Rg wave, numerical modeling

Introduction

Accurate discrimination of seismic events requires detailed knowledge of the propagation characteristics of seismic waves in a region. Presently, such propagation characteristics are reasonably well known for P and S waves; however, much work remains to be done regarding surface wave propagation. I have been exploring numerical modeling methodologies of the regional amplitude (1-5mb) to improve the discrimination of earthquakes and nuclear explosions. For that purpose, I use the recordings of nuclear tests, explosions, and earthquakes in North Korea recorded by stations in South Korea and China. I compare them to synthetic seismograms with the aim of find effective discriminants between nuclear explosions and earthquakes. The predicted P-wave amplitudes for explosions should be much larger than those for earthquakes across the body-wave spectra. However, regional waveform modeling by Walter et al. (2007) showed strong tectonic release from the May 1998 India test and very little tectonic release in the recent North Korea tests. However, using the limited regional data available, the behavior of the P/S discriminant is similar in both events.

Since the 1960s, comparing a Rayleigh-wave magnitude to the body-wave magnitude has been a robust method for discriminating earthquakes and explosions (Bonner et al., 2006; Bonner et al., 2011; Kremenetskaya et al., 2002). In this article, I analyze the Rayleigh-wave amplitude at different frequency ranges and examine the possibilities for discrimination using only the surface wave magnitudes. The results suggest that the estimate from Rayleigh waves for explosions is significantly greater than that for earthquakes. By focusing on regional recordings of surface waves, it might be possible to apply the Rg amplitude discriminant to low-magnitude events. Rg waves have been previously proposed (Kafka, 1990; Saikia, 1992). The different characteristics of Rg waves in explosion and

Manuscript received by the Editor May 8, 2014; revised manuscript received October 8, 2014.
1. Petroleum Technology Institute, Korea National Oil Corporation, Anyang 431-711, South Korea.

earthquake data that were discussed in the 1990s were mainly attributed to focal depth differences. However, the issue of focal depth can be neglected in North Korea because the focal depth of most events is sufficiently shallow to create surface waves. Numerical modeling methods can help discriminate between earthquakes and explosions because the strong P waves of explosions create strong Rayleigh waves.

Data

I use two explosions (EX1 and EX2) on June 26, 2001 (39.212°N, 125.383°E) and October 30, 2001 (38.748° N, 125.267°E), a nuclear test (NT) on October 9, 2006 (41.275°N, 129.095°E), and two earthquakes (EQ1 and EQ2) on April 14, 2002 (39.207°N, 125.686°E) and June 7, 2002 (38.703°N, 125.638°E), all in North Korea, to explore techniques for distinguishing between explosions and earthquakes in Korea (Tables 1 and 2). The epicenter of NT and the location of the recording stations are shown in Figure 1. This particular nuclear test of North Korea has been researched by many (e.g., Howard and Steven, 2008; Hong et al., 2008; Hong and Lee, 2009; Chun et al., 2011). The epicenters of the two explosions (EX1 and EX2) and two earthquakes (EQ1 and EQ2) and the location of the recording stations are shown in Figure 2.

Table 1 Focal parameters of explosions and earthquakes

Date	Lat. (N)	Long. (E)	mb
EX1 (June 26, 2001)	39.212°	125.383°	1.3
EX2 (October 30, 2001)	38.748°	125.267°	1.2
NT (October 9, 2006)	41.275°	129.095°	4.3
EQ1 (April 14, 2002)	39.207°	125.686°	2.1
EQ2 (June 7, 2002)	38.703°	125.638°	2.8

Analysis

The use of solutions in terms of the double integral transformation in the wavenumber and frequency domains (Hudson, 1969) have led to considerable progress in discriminating explosions from earthquakes. The relative amplitudes of the different phases in the data show the similarities and differences between explosions and earthquakes in the same area. There are several important aspects in the forward modeling of such data. One is the lack of detailed information regarding the

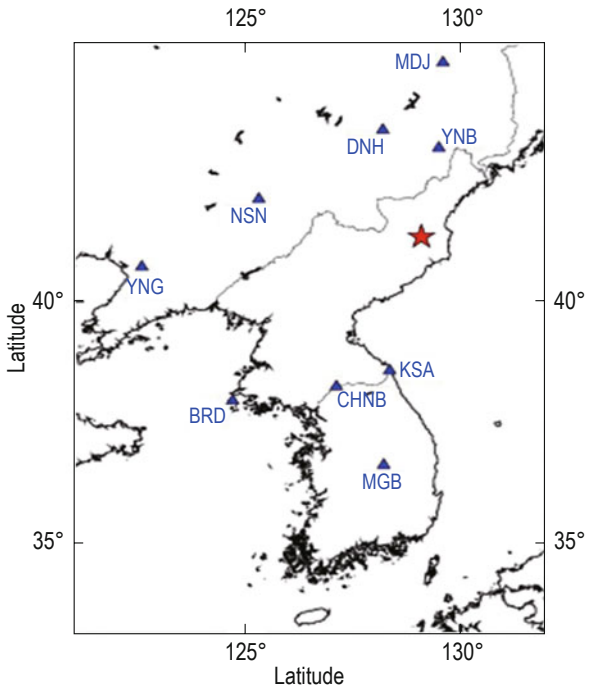

Fig.1 Recording stations (blue triangles) and the epicenter of the nuclear test (red star) at 41.275°N and129.095°E in North Korea on October 9, 2006.

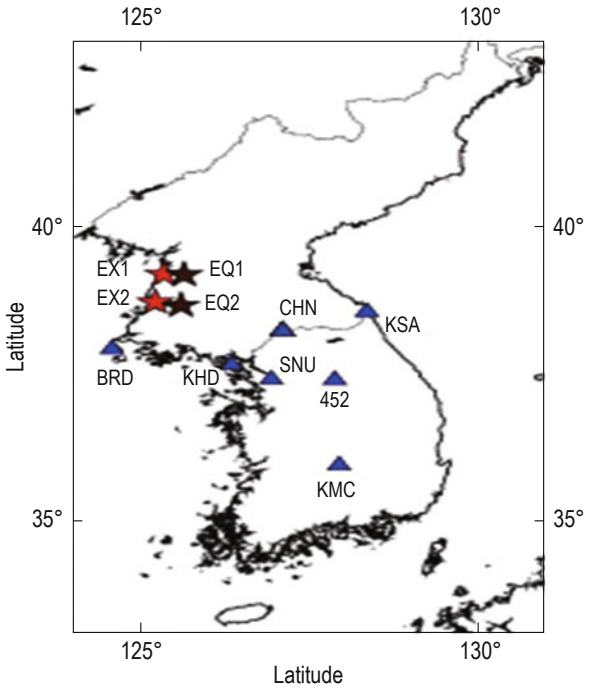

Fig.2 Recording stations (blue triangles) and the epicenters of the two explosions (red stars) on June 26, 2001 (EX1: 39.212°N, 125.383°E) and October 30, 2001 (EX2: 38.748°N, 125.267°E) and of the two earthquakes (black stars) on April 14, 2002 (EQ1: 39.207°N, 125.686° E) and June 7, 2002 (EQ2: 138.703°N, 125.638°E) in North Korea.

Table 2 Recording seismic stations used in this study

Station Code	Lat. (N)	Long. (E)	Velocity	Acceleration	Recorder	Period
452 (KSRS)	37.48333	127.90001	STS-2	ES-T	Q330HRS	Broadband
BGD	34.16003	126.55552	STS-2	ES-T	Q330HRS	Broadband
CHNB	38.27096	127.1211	CMG-3TB, STS-2	-	Q330S	Broadband
KHD	37.7036	126.3774	STS-2	ES-T	Q330HRS	Broadband
KMC	35.98692	127.94262	CMG-40T-1	ES-T	Q330HRS	Short
KSA	38.59532	128.3516	STS-2	ES-T	Q4128	Broadband
MGB	36.6402	128.2146	CMG-3TB	ES-DH	Q4128	Broadband
SNU	37.45363	126.95455	STS-2	ES-T	Q330HRS	Broadband
DNH	43.3446	128.1982	STS-2	-	-	Broadband
MDJ	44.617	129.591	STS-1V/VBB	FBA-23	Q330	Broadband
NSN	42.0183	125.3180	STS-2	-	-	Broadband
YNB	43.0029	129.4987	STS-2	-	-	Broadband
YNG	40.6836	122.6031	STS-2	-	-	Broadband

velocity structure in the area, and near the sources and the receivers. The forward model of Cho et al. (2011a) was used to fit the real data in this study, selected from the literature about the crustal structure of the Korean peninsula (Cho and Lee, 2006; Cho et al., 2007; Yoo et al., 2007; Cho et al., 2011a, 2011b; Cho, 2014). The expected amplitude of the vertical component of the first arrivals of the P and S waves strongly depends on the near-receiver structure. I looked for shapes, including the time and amplitude of synthetic seismograms, by varying the source mechanism, thickness, velocity, and the attenuation of the surface sedimentary layers.

Though it does not consider the possible local structures at the source and the receivers, the one-dimensional model of Cho et al. (2011a) offers detailed information of the upper crust, including sedimentary layers, obtained by surface wave analysis and trial-and-error forward modeling.

The real vertical-component data (KHDZ) recorded at the KHD station from EX1 are compared with the synthetic data generated from four source mechanisms, i.e., vertical strike slip (SS), 90° dip slip (DS), 45° dip slip, and explosion (EX). I obtain the focal mechanism by comparing the radial components of the real and synthetic data.

The amplitude ratio of P and S waves and surface waves in the vertical and radial components of the synthetic ZDS and RDS data, which are generated from the 90° dip slip source, is most similar to the real data in the vertical component of the KHD station, called KHDZ. The synthetic RDS data are closer to the real data than the synthetic ZDS data, whereas the absolute amplitude of the P waves at ZDS is greater and resembles more the real data than the absolute amplitude at RDS. However, the synthetic ZEX and REX data, which are generated from the explosion source, show larger surface wave amplitudes with clear dispersion. More simulation studies of the wave pattern of real data using explosion sources are clearly needed even though many models have been proposed to simulate the wave patterns of real data. The synthetic data for the vertical component of the 90° dip slip source at the two CHN stations, which consist of four short-period channels CHN03, CHN01, CHN00, and CHN02 and one broadband channel CHNB, and KHD, match the real data.

In contrast to explosions, real earthquakes data are difficult to simulate because, probably, data regarding the source mechanism of the earthquakes are lacking. To overcome this difficulty and obtain more reliable information on the source mechanism of the earthquakes, I vary the dip, slip, and strike at 10° intervals from 0° to 90° while simulating the real data of EQ1 recorded at the CHN02 station.

From the forward modeling, it can be observed that the shape of the synthetic seismogram is more sensitive to the slip angle than the strike or dip angle. If the slip angle or the dip angle is oblique, the energy of the first P waves is extremely weak. Hence, this may help to distinguish between explosions and earthquakes. Nonetheless, it is difficult to define clear criteria for distinguishing explosions from earthquakes with vertical strike slip or 90° dip slip. Considering the complexities of the waveforms in synthetic earthquake data, the EQ1 and EQ2 earthquakes and their focal mechanisms are simulated by comparing the real and synthetic data while varying the strike, slip, and dip angle. This requires less computational effort because of the assumption of a

simple focal mechanism while varying the angles. The wave phases are attributed to vertical discontinuities and regional surface variations.

Results

By comparing real and synthetic data, regional phases, such as Pg, Pn, Sn, Lg, and Rg, are picked in the vertical component of the NT seismic data at the recording stations (YNB, DNH, KSA, NSN, MDJ, CHNB, MDB, BRD, and YNG), as shown in Figure 3. In general, the recording signals of NT show the typical pattern of artificial explosions in which the amplitude of the P waves is greater than that of the S waves. All phases, except the Lg phase of the synthetic seismogram, well fit the real data. In theory, Lg waves are Love waves; thus, Lg waves cannot be observed in the vertical component. Nonetheless, Lg waves are observed owing to the scattering and conversion of the real data.

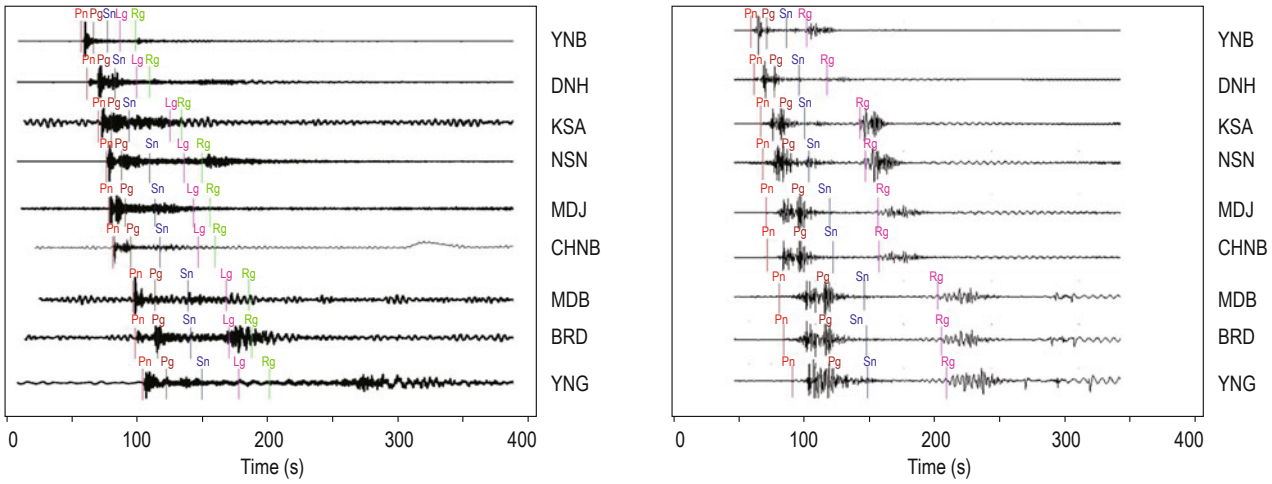

Fig.3 Vertical components of real seismic data (upper) and synthetic seismic data (lower), and picked phases in both data.

Studies of regional-scale waveforms typically suffer from uncertainties related to complications along the propagation path, such as three-dimensional scattering. Therefore, the Lg waves in the vertical component of real data are difficult to model. I used Pn of 7.5 km/s, Pg of 6.7 km/s, Sn of 4.4 km/s, and Rg of about 3.3 km/s to create synthetic seismograms to match the real data with the exception of the Lg waves. In the real seismic data, the velocity of the Lg phase is slightly faster than that of the Rg phase. In the real data of the BRD surface waves, the Lg and Rg waves are dominant compared with the other stations. This may imply the presence of a low-velocity, surface, sedimentary layer in the travel path to BRD. In Figure 4, the seismic data of NT recorded at YNG are filtered at different frequency bands. Pg waves clearly appear above 2 Hz and Rg waves clearly dominate at 0.05-2 Hz. In Rayleigh waves, the critically refracted P waves coexist with the incident SV wave. Free Rayleigh waves, which are coupled P–SV waves, travel along the surface with a velocity lower than the shear velocity. Because P waves are dominant in explosions, we may see

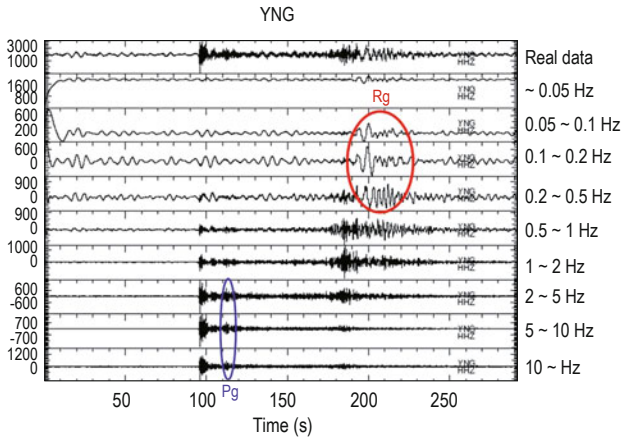

Fig.4 Real NT data recorded at the YNG station in Figure 1 and signals filtered at different frequency bands.

the dominant Rg waves from 0.05 to 2 Hz.

In the real and synthetic data, regional phases, such as Pg, Pn, Sn, Lg, and Rg, are picked at the vertical component of the EX1 seismic data at recording stations CHN03, CHNB, CHN01, CHN00, CHN02, and KHD,

as shown in Figure 5. In general, the recording signals of the explosion show the typical pattern of artificial explosions with P-wave amplitude significantly greater than the S-wave amplitude. Though the CHN03, CHNB, CHN01, CHN00, and CHN02 stations are very near, the depth of the sedimentary layers below each station affects the amplitude of the surface waves of the real data. For EQ1 that occurred near EX1, regional phases, such as Pg, Pn, Sn, Lg, and Rg, are picked at the vertical component of the EQ1 seismic data at the recording stations CHN03, CHNB, CHN01, CHN00, CHN02, KHD, 452BB, and KMC, as shown in Figure 6.

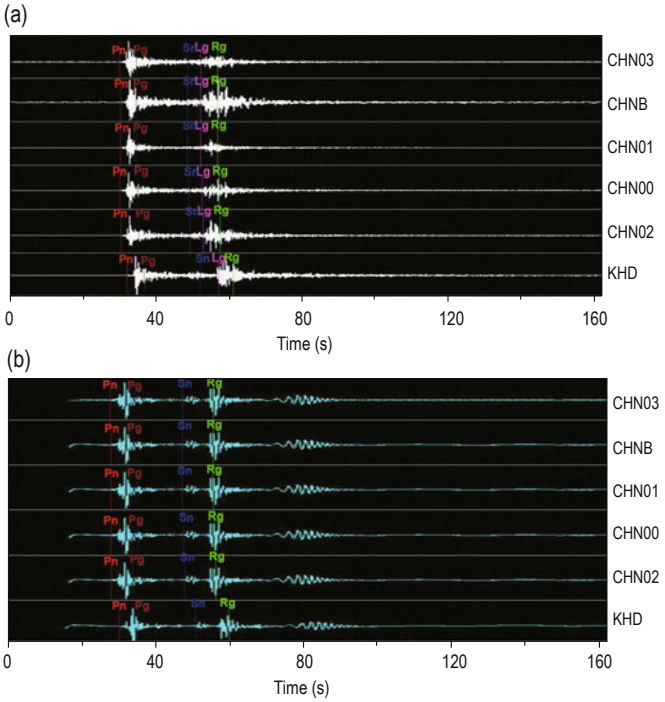

Fig.5 (a) Recordings of the vertical components of EX1 at the CHN03, CHNB, CHN01, CHN00, CHN02, and KHD stations from top to bottom, and picked Pn (red), Pg (brown), Sn (blue), Lg (pink), and Rg (green) phases. (b) Synthetic data most closely similar to the real data (a), stations CHN03, CHNB, CHN01, CHN00, CHN02, and KHD from top to bottom and picked Pn (red), Pg (brown), Sn (blue), and Rg (green) phases.

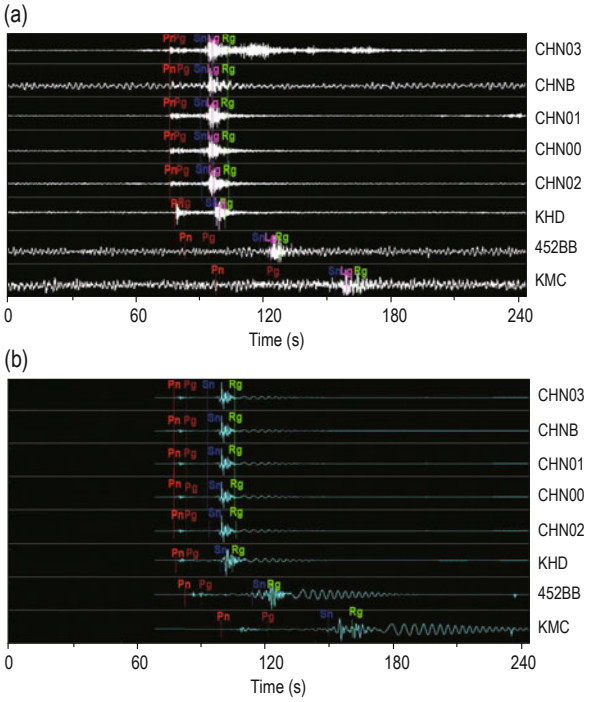

Fig.6 (a) Recordings of the vertical components of EQ1 at CHN03, CHNB, CHN01, CHN00, CHN02, KHD, 452BB, and KMC stations from top to bottom and picked Pn (red), Pg (brown), Sn (blue), Lg (pink), and Rg (green) phases. (b) Synthetic data most closely similar to the real in (a) at CHN03, CHNB, CHN01, CHN00, CHN02, KHD, 452BB, and KMC stations from top to bottom and picked Pn (red), Pg (brown), Sn (blue), and Rg (green) phases.

Discussion

In general, the recorded earthquake signals show the typical pattern of earthquakes in which the amplitude of S-phase waves is significantly higher than the P-wave amplitude. The real KHD data are characterized by P waves of higher energy than that of the other stations. In Figure 7, the real EX1 and EQ1 data recorded at CHNB are filtered using different frequency bands. Pg waves clearly appear above 2 Hz and Rg waves are clearly dominant at 0.05–0.5 Hz in the explosion data, whereas this is not seen in the earthquake data. Rg waves have been previously proposed as the final or main discriminant (Kafka, 1990; Saikia, 1992). Though the magnitude of the explosion and earthquake data in this study varies, the different characteristics of the Rg waves in the explosion and earthquake data are not attributed to the forward modeling of the magnitude variation.

To distinguish explosions and earthquakes in North Korea by comparing real and synthetic data, regional phases are picked in the vertical component of the EX2 seismic data at recording stations CHN03, CHNB, CHN00, CHN01, CHN02, SNU, 452BB, and KMC, as shown in Figure 8. The recorded signals of the explosion show the typical pattern of artificial explosions in the ratio of the amplitude of P and S waves. The real 452BB and KMC data of the relatively distant epicenter exhibit

large-amplitude Pg waves. For the earthquake near EX2, comparing real and synthetic data, regional phases are picked in the vertical component of the EQ2 seismic data at recording stations CHN03, CHN01, CHN00, CHN02, SNU, and 452BB, as shown in Figure 9. The recorded EQ2 signals show the typical amplitude ratio between P and S waves. In Figure 10, the real EX2 and EQ2 data at the SNU station are filtered at different frequency bands. Pg waves clearly appear above 2 Hz and Rg waves are clearly dominant at 0.2–2 Hz in the explosion data but not in the earthquake data.

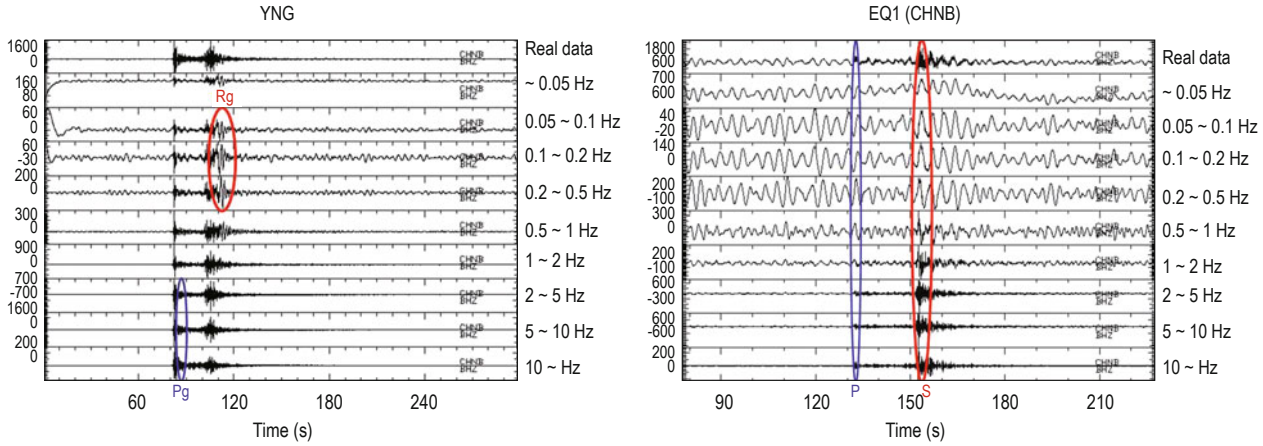

Fig.7 Real EX1 data (upper) and EQ1 (lower) recorded at the CHNB station in Figure 4 and signals filtered at different frequency bands for both EX1 and EQ1.

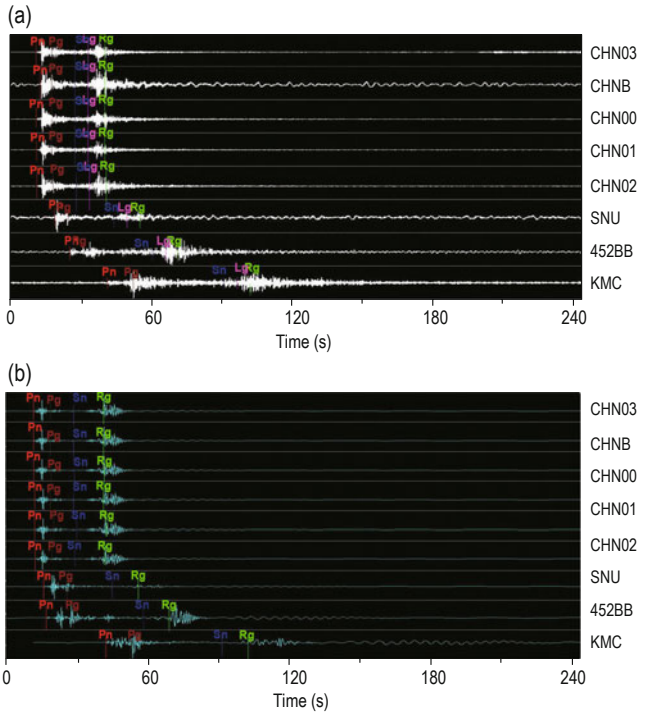

Fig.8 (a) Recorded data of the vertical component of EX2 at CHN03, CHNB, CHN00, CHN01, CHN02, SNU, 452BB, and KMC stations from top to bottom and picked Pn (red), Pg (brown), Sn (blue), Lg (pink), and Rg (green) phases. (b) Synthetic data most closely similar to the real data in (a) at CHN03, CHNB, CHN00, CHN01, CHN02, SNU, 452BB, and KMC stations from top to bottom and picked Pn (red), Pg (brown), Sn (blue), and Rg (green) phases.

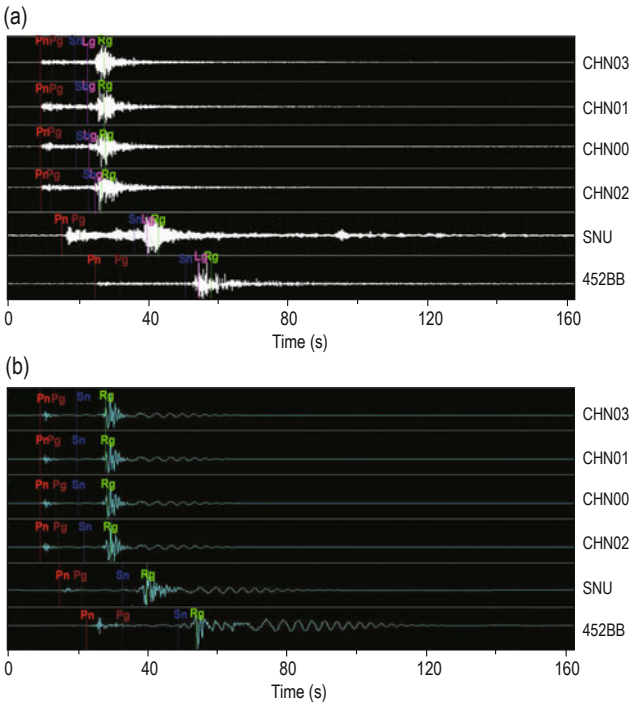

Fig.9 (a) Recorded data of the vertical component of EQ2 at CHN03, CHN01, CHN00, CHN02, SNU, and 452BB stations from top to bottom and picked Pn (red), Pg (brown), Sn (blue), Lg (pink), and Rg (green) phases. (b) Synthetic data most closely similar to the real data in (a) at CHN03, CHN01, CHN00, CHN02, SNU, and 452BB stations from top to bottom and picked Pn (red), Pg (brown), Sn (blue), and Rg (green) phases.

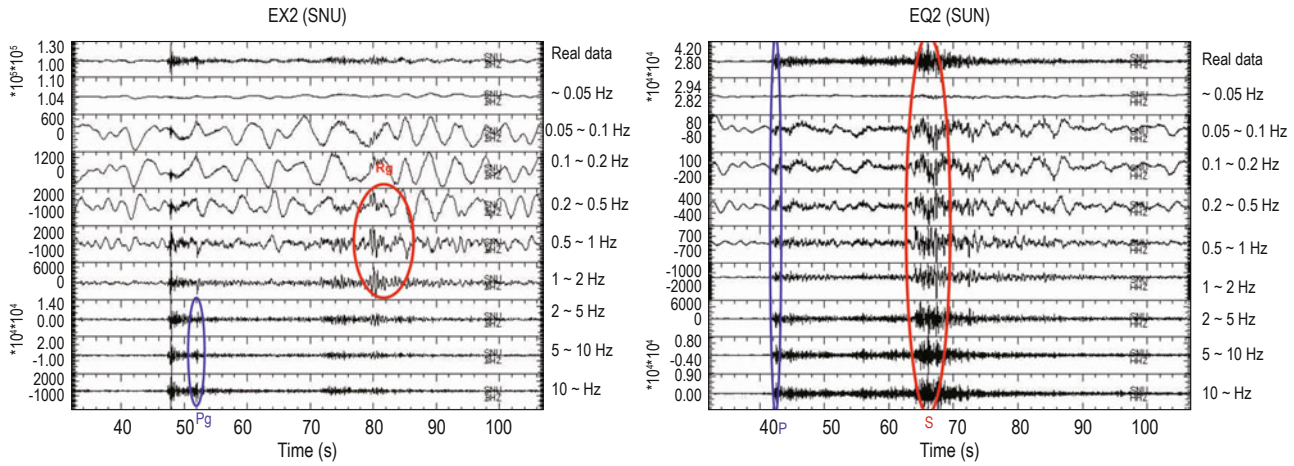

Fig.10 Real data of EX2 (upper part) and EQ2 (lower part) recorded at SNU and signals filtered at different frequency bands (0 – 0.05 Hz, 0.05 – 0.1 Hz, 0.1 – 0.2 Hz, 0.2 – 0.5 Hz, 0.5 – 1 Hz, 1 – 2 Hz, 2 – 5 Hz, 5 – 10 Hz, and above 10 Hz from top to bottom) for both EX2 and EQ2.

Conclusion

Earthquake, explosion, and a nuclear test data in North Korea have been compared with forward modeling and band-pass filtered surface wave amplitude data for discriminating earthquakes and explosions. The explosion signal has been characterized by first P waves with higher energy than that of S waves. Rg waves are clearly dominant at 0.05 – 0.5 Hz in the explosion data but not in the earthquake data, attributed to the dominant P waves in the explosion and their coupling with the SH components.

Acknowledgments

This study would not have been possible without the digital data sets provided by the Korean Institute of Geoscience and Mineral Resources. I also wish to thank the reviewers for their constructive comments.

References

Bonner, J., Russell, L., Harkrider, D., Reiter, D., and Herrmann, R., 2006, Development of a time-domain variable period surface wave magnitude measurement procedure for application at regional and teleseismic f America, **96**, 678–696.

Bonner, J., Stroujkova, A., and Anderson, D. N., 2011, Improving earthquake and explosion discrimination by using Love and Rayleigh wave magnitudes, in "2011 Monitoring Research Review: Ground-Based Nuclear Explosion Monitoring Technologies" sponsored by the Air Force Research Laboratory.

Cho, K. H., and Lee, K., 2006, Dispersion of Rayleigh waves in the Korean Peninsula: Journal of the Korean Geophysical Society, **9**, 231–240.

Cho, K. H., Herrmann, R. B., Ammon, C. J., and Lee, K., 2007, Imaging the upper crust of the Korean Peninsula by surface wave tomography: Bulletin of the Seismological Society of America, **97**, 198–207, doi: 10.1785/0120060096.

Cho, K. H., Lee, S.-H., and Kang, I. -B., 2011a, Crustal structure of the Korean Peninsula using surface wave dispersion and numerical modeling: Pure and Applied Geophysics, **168**, 1587–1598, doi: 10.1007/s00024-011-0262-x.

Cho, K. -H., Chen, H. W., Kang, I. -B., and Lee, S. -H., 2011b, Crust and upper mantle structures of the region between Korea and Taiwan by surface wave dispersion study: Geoscience Journal, **15**, 71–81, doi: 10.1007/s12303-011-0009-9.

Cho, Kwang Hyun, 2014, Discovery of a surface-wave velocity anomaly in the West Sea of South Korea: Exploration Geophysics, **45**, 86–93.

Chun, K. -Y., Wu, Y., and Henderson, G. A., 2011, Magnitude estimation and source discrimination: A close look at the 2006 and 2009 North Korean underground nuclear explosions : Bulletin of the Seismological Society of America, **101**, 1315–1329.

Hong, T. -K., Baag, C. -E., Choi, H., and Sheen, D. -H, 2008, Regional seismic observations of the 9 October

2006 underground nuclear explosion in North Korea and the influence of crustal structure on regional phases: Journal of Geophysical Research, **113**, B03305, doi: 10.1029/2007JB004950.

Hong, T. -K. and Rhie, J., 2009, Regional source scaling of the 9 October 2006 underground nuclear explosion in North Korea: Bulletin of the Seismological Society of America, **99**, 2523–2540.

Howard J. P., and Steven, R. T., 2008, Effects of shock-induced tensile failure on mb-Ms discrimination: Contrasts between historic nuclear explosions and the North Korean test of 9 October 2006, Geophysical Research Letters: **35**, L14301, doi: 10.1029/2008GL034211.

Hudson, J. A., 1969, A quantitative evaluation of seismic signals at teleseismic distances II. Body waves and surface waves from an extended source: Geophys. J., **18**, 353–370.

Kafka, A. L., 1990, Rg as a depth discriminant for earthquakes and explosions - a case study in New England: Bulletin of the Seismological Society of America, **80**, 373–394.

Kremenetskaya, E., Asming, V., Jevtjugina, Z., and Ringdal, F., 2002, Study of regional surface waves and frequency-dependent Ms:mb discrimination in the European Arctic: Pure and Applied Geophysics, **159**, 721–733.

Saikia, C. K., 1992, Numerical Study of Quarry Generated Rg as a Discriminant for Earthquakes and Explosions - Modeling of Rg in Southwestern New England: Journal of Geophysical Research, **97**, 11,057-11,072.

Walter, W. R., Matzel, E., Pasyanos, M., Harris, D. B., Gok, R., Ford, S. R., 2007, Empirical observations of earthquake-explosion discrimination using P/S ratios and implications for the sources of explosion S-waves: "MRR2007-29th Research Review on Nuclear Explosion Monitoring Technologies" sponsored by the Air Force Research Laboratory.

Yoo, H. J., Herrmann, R. B., Cho, K. H., and Lee, K., 2007, Imaging the three-dimensional crust of the Korean Peninsula by joint inversion of surface-wave dispersion and teleseismic receiver functions: Bulletin of the Seismological Society of America, **97**, 1002–1011, doi: 10.1785/0120060134.

Cho, Kwang-Hyun obtained his M.S. (2001) and Ph.D. in Seismology from Seoul National University (2006). After one year postdoctoral research at KIGAM, Korea Institute of Geoscience and Mineral Resources, he joined the Korea National Oil Corporation (KNOC) in 2006. His research interests are applied earthquake seismology, seismic numerical modeling, seismic wave propagation, and surface wave tomography including ANT (Ambient Noise Tomography).